JOURNAL OF APPLIED ELECTROCHEMISTRY 14 (1984) 23–37

A hybrid method through Faradaic rectification and a.c. impedance measurements for the corrosion rate determination of metal/oxide/electrolyte systems. II. Experimental results for anodized aluminium

C. S. C. BOSE, R. SRINIVASAN*

Department of Chemistry, Indian Institute of Technology, Powai, Bombay 400 076, India

Received 25 January 1983

An experimental verification of a method for the determination of the corrosion rate of metal/oxide/electrolyte systems, using both faradaic rectification and a.c. impedance measurements, is reported using zone refined aluminium electrodes in 1 mol dm^{-3} aqueous sodium sulphate at pH 1.9. The impedance and the rectification parameters due to the anodic oxide on the electrode have also been computed and used to determine instantaneous corrosion rate of the same system at different values of the pH. The direction and magnitude of rectification by this system are found to be sensitive to pH as well as dissolved oxygen in the electrolyte. They are explained by a decrease in equilibrium exchange current for the hydrogen evolution reaction with increase in pH and an inhibitive effect of oxygen on the former reaction.

1. Introduction

Aluminium and its alloys occupy an important place in modern technology. Besides being excellent structural materials, they have many uses in different fields, such as, sacrificial anodes, battery electrodes, and in the electronic and printing industries.

The corrosion behaviour of aluminium is almost unique, barring only magnesium. In terms of both thermodynamics and kinetics aluminium should be an extremely unstable element when exposed to ambient conditions. The instability of the metal leads to the formation of aluminium oxide. This oxides settles on the surface of the metal, protecting the substrate from all oxidizing agents, and making it far more stable than expected. All attempts to protect the metal from corrosion, by way of alloying, anodizing and other methods of surface finishing are only aimed at enhancing the stability of the surface oxide. This oxide is by and large a poor conductor of electricity (specific resistance $\simeq 10^{13}\,\Omega\,m$). As a result, electrochemical methods cannot be employed for accurate evaluation of the corrosion rate. Nevertheless, a large number of these methods, ranging from the conventional logarithmic/linear polarization to the more recent a.c. impedance are being employed for this purpose. All these methods had originally been proposed only for metal/electrolyte rather than metal/oxide/electrolyte systems. When they are employed in the latter type of systems, such as an aluminium electrode immersed in acidic or neutral electrolyte, only an order of magnitude of the corrosion rate could, at best, be obtained. Moreover it is doubtful whether the mechanism of corrosion can be found by employing such techniques with oxide covered metal electrodes.

A brief review has recently been made of the existing electrochemical methods and their limitations when applied to metal/oxide/electrolyte systems [1]. The same communication also describes the theory for a new approach which overcomes those limitations. The newly proposed method is essentially based on combining two well known techniques in electrochemistry, namely,

* To whom communications should be addressed.

0021–891X/84 $03.00 + .12.

faradaic rectification and a.c. impedance, but with certain important modifications. A brief summary of the proposed theory is given below. An experimental verification of the theory, using the anodized aluminium electrode, is also provided.

2. Theory

The model of corrosion may be represented by the following simultaneous reactions at the metal/oxide/electrolyte system

$$M \rightarrow M^{+n} + ne^- \quad (1)$$

$$O + ne^- \rightarrow R \quad (2)$$

These two reactions can occur at any one or both of the two interfaces, i.e. the metal/oxide and/or the oxide/electrolyte. This leads to four different combinations by which they can occur simultaneously.

The electric field that exists in the system consists of two components: (i) across the oxide film and (ii) across the reaction planes* (or the two interfaces). The entire field normally measured in terms of electrical potential, E (against any given reference electrode) is also considered to have two components i.e. E^{Fl} and E^r (E is an experimentally measurable quantity whereas E^{Fl} and E^r are not).

The rate of charge transfer reactions across the interfaces follow the usual laws of electrode kinetics. Across the bulk of the oxide, conduction is by ions, electrons and/or holes and the currents are exponentially related to the field across the oxide [2].

When an alternating voltage of amplitude V_p is applied across the electrochemical cell such that a small amplitude alternating potential $[E_p \cos(\omega t - \phi)]$ is incident across the metal/oxide/electrolyte system, a net current (i), which is a sum of an alternating current ($\tilde{i}$) and a direct current ($\bar{i}$), passes through it. $\bar{i}$ is the result of faradaic rectification (due to Reactions 1 and 2), besides any possible rectification due to the bulk of the oxide. Under these conditions, the rest potential (E_{cor}) shifts to a new value (E_1). When $\bar{i}$ is off-set to zero, with no change in V_p and $\tilde{i}$, E_1 changes to E_2.

Of the total potential $[E_p \cos(\omega t - \phi)]$ incident across the system, one part is dropped across the oxide film $[E_p^{Fl} \cos(\omega t - \hat{\phi})]$ and the other across the two interfaces $[E_p^r \cos(\omega t - \theta)]$. So are E_{cor}, E_1 and E_2 in terms of the oxide film (E_{cor}^{Fl}, E_1^{Fl} and E_2^{Fl}) and the reaction planes (E_{cor}^r, E_1^r and E_2^r).

Under the above conditions the following relations are valid

$$i_{cor} = \frac{\bar{i}}{2(\eta_2^r - \eta_1^r)[K\alpha^r - 2\eta_2^r/(E_p^r)^2]} \quad (3)$$

$$(\eta_2 - \eta_1) = \frac{\bar{i}}{i_{cor}(k+1)} x + (\eta_2^r - \eta_1^r) \quad (4)$$

$$\eta_2^r = (\eta_2^r - \eta_1^r) + \eta_1 + \bar{i}|Z_{Fl}| \quad (5)$$

$$(\eta_2 - \eta_1) = (\eta_2^{Fl} - \eta_1^{Fl}) + (\eta_2^r - \eta_1^r) \quad (6)$$

$$\eta_1 = E_1 - E_{cor} \quad (7)$$

$$\eta_2 = E_2 - E_{cor} \quad (8)$$

$$\eta_1^r = E_1^r - E_{cor}^r \quad (9)$$

$$\eta_2^r = E_2^r - E_{cor}^r \quad (10)$$

$$E_p^2 = V_p^2 + (i_p R_\Omega)^2 - 2V_p i_p R_\Omega \cos\hat{\theta} \quad (11)$$

and

$$(E_p^r)^2 = E_p^2 + [i_p|Z_{Fl}|]^2 - 2E_p i_p |Z_{Fl}| \cos(\hat{\phi} - \phi) \quad (12)$$

where i_{cor} is the corrosion current; k and l are constants dependent on film properties; $|Z_{Fl}|$ is the impedance of the oxide film of thickness x; $K\alpha^r = 2.303/b_c^r$, where b_c^r is the apparent Tafel slope at $x = 0$. (See Appendix I of [1] for more details on $K\alpha^r$.) i_p in Equations 11 and 12 is the (peak) amplitude of the alternating current ($\tilde{i}$) through the cell; $\hat{\theta}$, ϕ and $\hat{\phi}$ are the phase shifts between i_p and V_p (across the cell), E_p (across the working electrode) and E_p^{Fl} (across the oxide film) respectively; R_Ω is the resistance due to the electrolyte between the working electrode and the counter electrode.

As may be observed from Equation 4, $(\eta_2^r - \eta_1^r)$ is computed from $(\eta_2 - \eta_1)$, after determining the latter at different values of x but at a constant $\bar{i}$ (at which i_{cor} in Equation 3 is to be determined). It is assumed here that $(\eta_2^r - \eta_1^r)$ as well as i_{cor}, k

* In the present analysis the field across the diffuse layer is considered as a part of the reaction-plane field. The 'IR drop' across the electrolyte and the reference electrode is left to be minimized by appropriate positioning of the Luggin tip of the reference electrode.

and l are independent of x. (This may, however, be true only over a small range of x.)

η_2^r is determined according to Equation 5.

E_p^r, the (peak) amplitude of the alternating potential across the reaction planes, is computed from the measured value of V_p after a vectorial subtraction of the potential drop across the electrolyte resistance, R_Ω and the oxide film impedance, $|Z_{Fl}|$.

$|Z_{Fl}|$, unlike the cell impedance, $|Z_t|$, may not be accessible to direct measurements. Further, $|Z_{Fl}|$ could depend on the frequency of measurement and in a manner very different from $|Z_t|$. It will therefore need to be computed from $|Z_t|$ at the angular frequency, ω, at which the faradaic rectification measurements are made. The procedure described elsewhere [3] may be followed for this purpose.

Further, from Equation 6 $(\eta_2^{Fl} - \eta_1^{Fl})$ can be determined at any given value of x for a set of $\bar{i}$. This, together with $|Z_{fl}|$ at that value of x, should form a set of parameters, the values of which are intrinsic to the given oxide film. Once these values are obtained for a given electrode (in a given electrolyte, say, which is 'inert', i.e. does not corrode the test electrode or dissolve the oxide film to any extent), it should be possible to evaluate its i_{cor} in any other electrolyte from only one set of faradaic rectification data; the elaborate procedure to determine $(\eta_2^{Fl} - \eta_1^{Fl})$ (following Equations 4 and 6) and $|Z_{Fl}|$ (following [3]) need not be repeated again.

3. Experimental details

Zone refined aluminium (purity = 99.9999%) was used as the test electrode. It was held in a push-fit Teflon holder exposing only a disc like surface of area $1.96 \times 10^{-5}\,m^2$. A Hg/Hg_2SO_4/electrode formed the reference electrode without a liquid junction. Either a platinized platinum electrode (for impedance measurements) or a large area flat plate aluminium electrode (for rectification measurements) formed the counter electrode.

An electrochemical cell similar to the one described in Fig, 3 of [3] was used in the present study. However, the cell also had a piece of permanent magnet encapsulated in Teflon and was used for stirring the electrolyte during the rectification measurements.

Sodium sulphate ($1\,mol\,dm^{-3}$), with its pH adjusted to 1.9 by addition of sulphuric acid, was used as the test electrolyte. It was prepared from reagent grade chemicals, recrystallized from double distilled water.

The solution was nitrogen saturated for more than an hour and the temperature maintained at $25 \pm 1°C$.

For impedance measurements, the circuit described in Fig. 4 of [3] was adopted.

The test circuit used for faradaic rectification measurements is shown in Fig. 1. It is almost similar to the one proposed originally by Sathyanarayana [4], but with a minor modification. The resistances R_1, R_2 and R_3 along with the d.c. power supply (U) form the 'd.c. off-set' loop. (By adjusting the value of the variable resistance R_2 as well and the polarity of U, the d.c. current in the loop and thus the d.c. potential drop across R_3 were adjusted. This drop was used to off-set the d.c. rectification current ($\bar{i}$) in the main circuit.) It may be observed that R_3 has a fixed value (24 Ω) as against a variable one in the original circuit [4]. This modification was essential because it was mandatory to keep constant the resistance/impedance of all the components in the faradaic rectification circuit, except the impedance due to the cell itself. The latter, however, was varied (by producing oxide films of different thickness on the electrode surface) and their absolute values determined; this was a part of the experimental procedure.

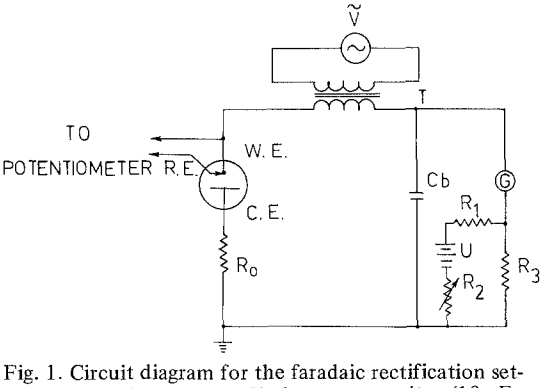

Fig. 1. Circuit diagram for the faradaic rectification set-up. G, d.c. galvanometer; Cb, by-pass capacitor (10 μF, polystyrene, low loss); U – NiCd cells (60 AHr at 70% state of charge) for the constant current offset circuit; WE, working electrode; CE, counter electrode; RE, reference electrode; R_1, 51 Ω resistance; R_2 variable decade resistance with a total resistance of 99999.9 Ω; R_3, 24 Ω resistance (non inductive); R_0, 10 Ω resistance (non inductive); $\tilde{V}$, oscillator T, shielded transformer.

The frequency of the test signal was 30 Hz. The choice of this frequency, discussed by Sathyanarayana [4], included a consideration of the simple circuit for the faradaic rectification measurement, non-interference of high frequency electrical noise, etc.

3.1. *Procedure*

The electrode surface was prepared and anodized following the procedure described earlier [3]. The electrode was always anodized in nitrogen saturated 1 mol dm^{-3} sulphuric acid. The acid was then pumped out, the cell washed with deaerated double distilled water and the test electrolyte pumped in. All these operations were done under nitrogen pressure and the anodized surface of the electrode never came in contact with the outside atmosphere.

The electrode was then given a cathodic polarization treatment at 30 A m^{-2} current for 150 min. Impedance and faradaic rectification measurements were commenced within 30 min after the cathodic polarization treatment. The cathodic polarization treatment was given in order to remove the traces of (adsorbed) oxygen left in the system after deaeration (see also Section 4.5).

The range of anodization potential covered was 5 to 14 V, corresponding to the oxide film thickness (x) of 9.2 to 20.4 nm. ($x = 1.245\ \text{V} \times 10^{-9} + x_i$; x_i is the thickness of the initial oxide film and equal to 3 nm.)

At least two sets of faradaic rectification and impedance measurements were carried out at each anodization voltage and the average value noted.

Galvanostatic cathodic polarization experiments (for the evaluation of $K\alpha^r$ in Equation 3) were conducted separately. The electrode preparation was the same as that described above.

3.2. *pH dependent studies*

Faradaic rectification measurements were also made on the zone refined aluminium electrode in 1 mol dm^{-3} sodium sulphate electrolyte at different values of pH. The range of pH covered was 0.9 to 6. However, the thickness (x) of the oxide film was always constant at 8 nm (4 V anodized), with the other conditions such as cathodic polarization treatment, etc. the same as in Section 3.1.

4. Results and discussions

4.1. *Cathodic polarization*

The $K\alpha^r$ value was derived from the steady state galvanostatic Tafel plot curves shown in Fig. 2. The solid lines in the figure represents the polarization curve for a 10 V anodized zone refined aluminium electrode ($x = 15.5$ nm). It is also the typical behaviour of the electrode at all other anodizing voltages in the range of 5–16 V, and only the linear part of the far-cathodic region of the final sweep is shown for the purpose of clarity. (In all these cases the potential scale is also shifted by a constant value). The apparent limiting current and the hysteresis of polarization which tends to shift after each 'sweep' is very similar to the one observed earlier in the case of the zinc/potassium hydroxide system [5, 6]. There the behaviour was explained by a slow adsorption–desorption phenomenon involving the cations [5] or the implantation of the alkali metal cation on the electrode surface [6]. A similar conclusion may be possible with the aluminium electrode. The absence of any limiting current or hysteresis with the aluminium electrode (anodized at 10 V) in sulphuric acid of pH 1 (shown by dotted lines in Fig. 2) also seems to support this view.

An interesting aspect here is that the polarization curves are identical at all anodizing voltages with the slopes of the Tafel lines falling in the range 0.19 ± 0.01 V. This apparently implies that either there is little potential drop across the oxide film or the variation in the potential with the thickness (x) of the oxide film is negligible. This is in total contradiction with our earlier expectations (cf. Appendix 1 of [1]) as well as by others. (Although Vijh [7] and Mayor [8] have not stated anything about the variation in the potential drop, with the thickness of the oxide film, it is implicit in their explanation about the high Tafel slopes observed on oxide covered metals.) Moreover, the distinct increase in the cell impedance, $|Z_t|$, with x observed at 30 Hz (see Fig. 4) and also at other frequencies in the range of $10–10^5$ Hz [3], seems to contradict the d.c. polarization (zero frequency?) observation. (But

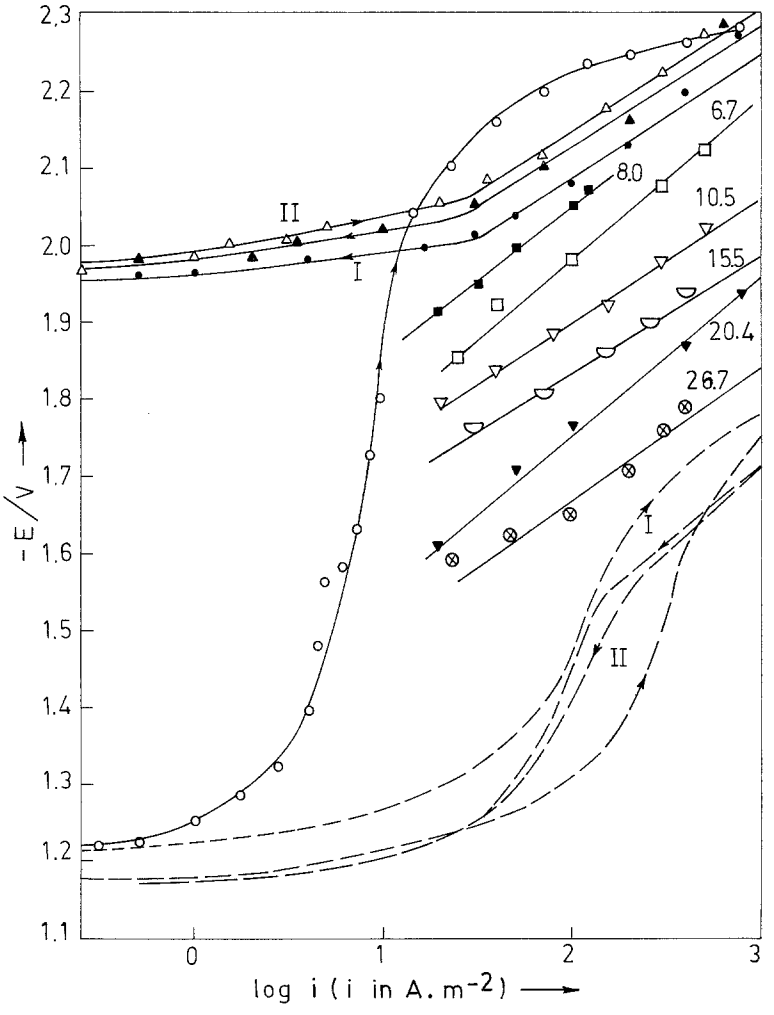

Fig. 2. Cathodic polarization curves for aluminium/oxide/1.0 mol dm^{-3} sodium sulphate. Numbers on the curve represent the thickness (x) of the oxide film in nm. Forward and reverse 'sweeps' of the I and II cycle shown only for the electrode with an oxide film of x = 15.5 nm (see text for details). Dotted line shows the cathodic polarization curve for the aluminium electrode in sulphuric acid (pH = 1).

there is apparently no direct or indirect evidence for the oxide film impedance and its mechanism of conduction in metal/oxide/electrolyte systems at zero frequency.)

The d.c. cathodic polarization inevitably leads to evolution of hydrogen in relatively large amounts (as compared to the small amplitude a.c. signals for shorter periods employed during rectification/impedance studies). This could lead to a large increase in the activity of hydrogen ion, atoms and molecules inside the oxide lattice as observed earlier by Ahmed [9]. The presence of hydrogen in any form may be expected to modify greatly the electric field in the oxide film, as in the case of titanium oxide [10].

For the purpose in hand, the average slope in the farcathodic region (0.19 V) was taken as b_c^r, the apparent slope at zero thickness of the oxide, and $K\alpha^r$ (equal to $2.303/b_c^r$) as 12.12.

4.2. *Evaluation of the corrosion rate at pH 1.9*

The variation of the rest potential (E_{cor}) of the anodized electrode with time (t) in the test electrolyte is shown in Fig. 3. These variations were almost independent of x and hence only the one corresponding to an electrode with x = 8.0 nm is shown in the figure. (In all cases E_{cor} stabilized between −1.17 and −1.27 V.) The impedance due to the cell, $|Z_t|$ was also monitored simultaneously and shown in the same figure. It may be seen that both E_{cor} and $|Z_t|$ stabilize simultaneously after about 150 min (at which point the faradaic rectification measurements were started).

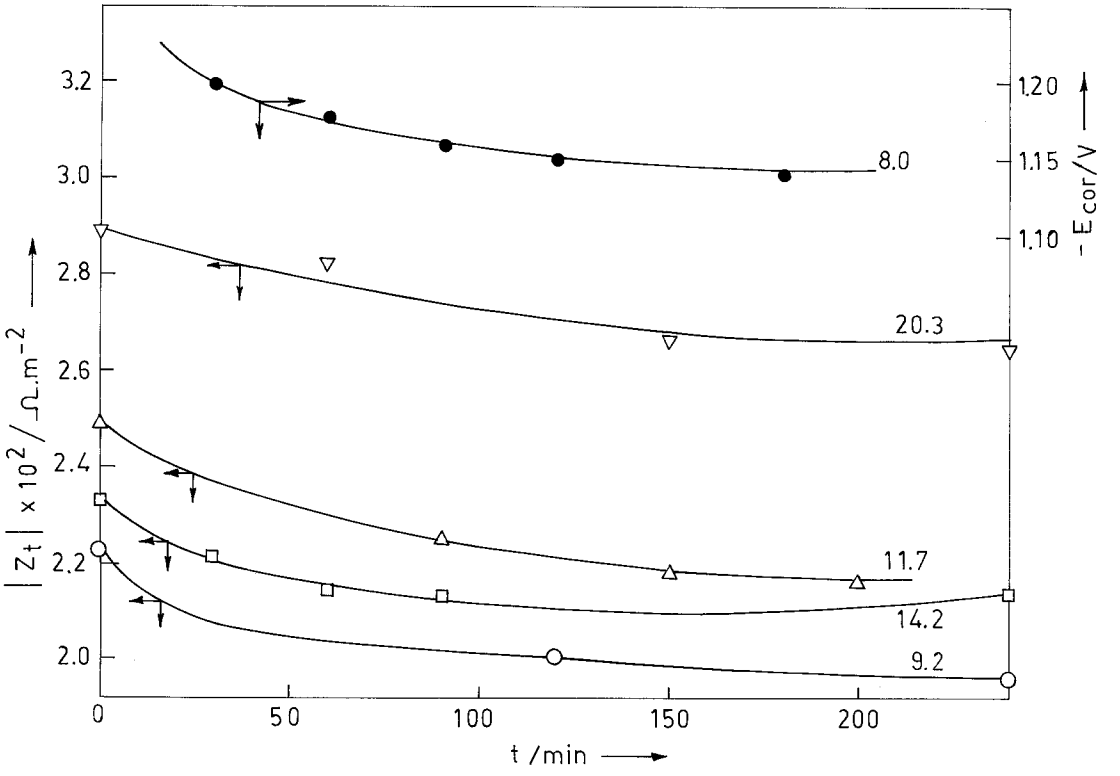

Fig. 3. Variation of E_{cor} and $|Z_t|$, with time. System: Zone refined aluminium/oxide/1 mol dm^{-3} sodium sulphate (pH = 1.9). Numbers on the curves denote x in nm.

Although E_{cor}, once stabilized were found to be independent of the thickness (x) of the oxide film, the cell impedance, $|Z_t|$, may be observed to depend on it. The stable values of $|Z_t|$ are plotted against x (Fig. 4). From the slope of this plot, the value of the film impedance $|Z_{Fl}|$ as well as the phase shift ($\hat{\phi}$) due to it at different values of x were computed, following the procedure described earlier [1, 3]. The computed values are also shown in Fig. 4.*

The experimental faradaic rectification data for the electrode at different thickness of the anodic oxide are summarized in Figs. 5 to 7. (The numbers on the curves represent the values of x).

* The small values of $|Z_{Fl}|$ at any given x as compared to the one reported earlier for zone refined aluminium [3], is clearly due to the effect of the 150 min cathodic polarization treatment followed in the present work (see also Section 4.1 for the effect of hydrogen on the conductivity of aluminium oxide). Cathodic reduction of aluminium oxide may, however, be ruled out due to the small overvoltage (ca. — 0.3 V) from E_{cor} registered during the polarization treatment, as compared to the large value of Nernst reversible potential of Al/Al^{+3}, i.e. about —1.1 V away from E_{cor}.

Figure 8 shows the variation of $(\eta_2 - \eta_1)$ with x at different values of $\bar{i}$, as computed from the data in Figs. 5–7†. From this $(\eta_2^x - \eta_1^x)$ was obtained as its intercept at $x = 0$, at each $\bar{i}$, (cf. Equation 4), and substituted in Equation 3 for the calculation of i_{cor} (see also Table 2). This was done following a least squares curve fitting method.

The electrolyte resistance (R_Ω), the phase shifts, ϕ and $\hat{\theta}$, are shown in Table 1. (They were all found to be almost independent of x, and hence, only the data corresponding to an electrode anodized at 5 V ($x = 9.2$ nm) is shown in the table).

The corrosion current, i_{cor}, was computed, using an EC-1030 computer, for the four values of x shown in Figs. 5 to 7 and for a set of five values of $\bar{i}$ (0.03–0.06 A m^{-2}) at each x. i_{cor} was found to be in the range of 2.56 to 5.56 A m^{-2}, with the average of the 20 values at 4.00 A m^{-2}. A few representative values are shown in Table 2.

† $\bar{i}$ was found to be extremely sensitive to pH (cf. Section 4.4 and Fig. 15) as much as it was to x. Hence, care should be taken to maintain the pH of the test electrolyte a constant.

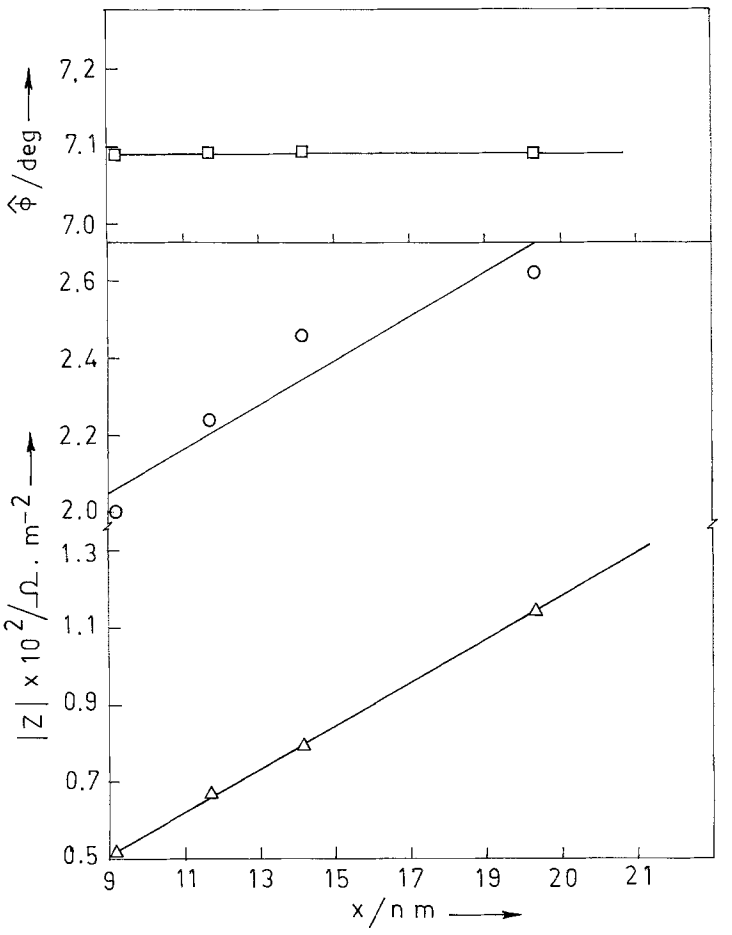

Fig. 4. Variation of $|Z_t|$ (shown as ○–○), $|Z_{F1}|$ (shown as △–△) and phase shift across the film ($\hat{\theta}$) with x. System: Same as in Fig. 3.

It may be seen from Table 2 that the values of i_{cor} are more or less identical at all values of x. This implies that the range x used to determine i_{cor}, were reasonable; the interfacial properties were only slightly affected by such small variations in x.

The reasonable linearity of $(\eta_2 - \eta_1)$ against x curves at various values of $\bar{i}$ in Fig. 8, as well as $|Z_t|$ against x curves in Fig. 4, may be taken as experimental proof of the validity of the assumptions made in the theory (see Sections 3.3, 3.4 and 3.5 in [1] for the assumptions).

4.3. *Effect of pH on the corrosion rate*

Experimental data on faradaic rectification of the 4 V anodized ($x = 8$ nm) electrode is summarized in Figs. 9 to 11. (The numbers on the curve represent the different pH values at which the measurements were made.)

Figure 12 shows the variation of rectification potential $(\eta_2^{F1} - \eta_1^{F1})$ with rectification current $(\bar{i})$ for the 8 nm thick oxide film. The points shown in the Figure were computed using the faradaic rectification data shown in Figs. 5 to 7; the solid line was drawn by a least squares curve fit procedure.

The impedance due to the 8 nm thick oxide film was computed as $4.50 \times 10^{-3}\ \Omega\,m^{-2}$ from Fig. 4. With the above data on the oxide film, $(\eta_2^r - \eta_1^r)$, η_2^r and E_p^r were computed at different values of the pH using Equations 5, 6, 10 and 12 and the data in Figs. 9 to 11. The corrosion current, i_{cor} was then calculated using Equation 3.

Figure 13 shows the calculated values of i_{cor} as a function of pH. It may be observed that i_{cor} increases with hydrogen ion concentration. Since hydrogen ion reduction forms the half-cell couple of the conjugate reaction, it may be concluded that the rate of this reaction also controls

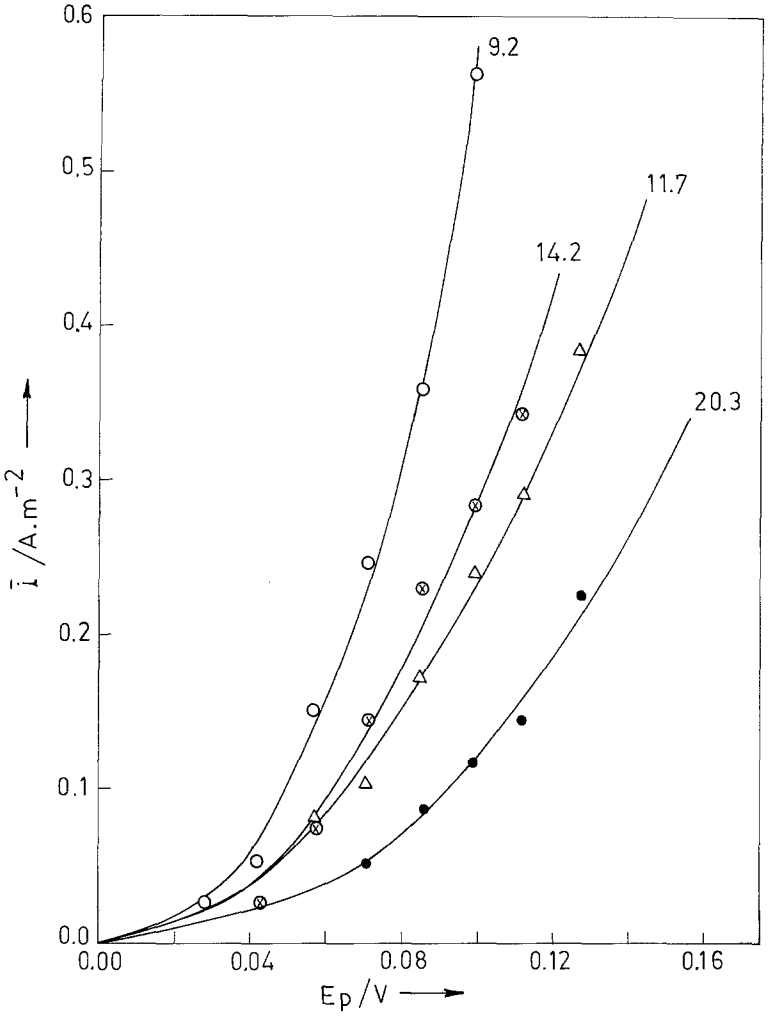

Fig. 5. Dependence of $\bar{i}$ on E_p. System: Same as in Fig. 3.

the overall rate of corrosion of the aluminium electrode.

4.4. *Effect of pH on the direction of rectification*

It may be seen from Fig. 9 that the sign of the rectification current, $\bar{i}$, depends on the pH. Using this data, $\bar{i}$ values were obtained at different pH, at a constant E_p (70 mV) and shown in Fig. 14. Thus, $\bar{i}$ was found to be cathodic (sign-positive, as

Table 1. Experimental data on the electrolyte resistance (R_Ω), phase shifts $\hat{\theta}$, between i_p and V_p and ϕ, across i_p and E_p, for 5 V anodized ($x = 9.2$ nm) electrode

$R_\Omega(\Omega)$	$\hat{\theta}$ (deg)	ϕ(deg)
7.0	63.22	63.64

Table 2. Computed values of the corrosion current for zone refined aluminium in 1 mol dm^{-3} sodium sulphate (pH = 1.9)

Oxide film thickness (x) (× 10^{10} m)	*Corrosion current* (i_{cor}) in A m^{-2} at	
	$\bar{i} = 0.0310$	$\bar{i} = 0.0612$
92.25	5.510	2.800
117.00	4.990	2.561
142.00	5.410	2.791
167.00	5.560	2.952
203.00	5.150	2.601

The value of
$(\eta_2^r - \eta_1^r) = 0.270 \times 10^{-3}$ V at
$\bar{i} = 0.031$ A m^{-2}
and
$= 0.107 \times 10^{-2}$ V at
$\bar{i} = 0.061$ A m^{-2}

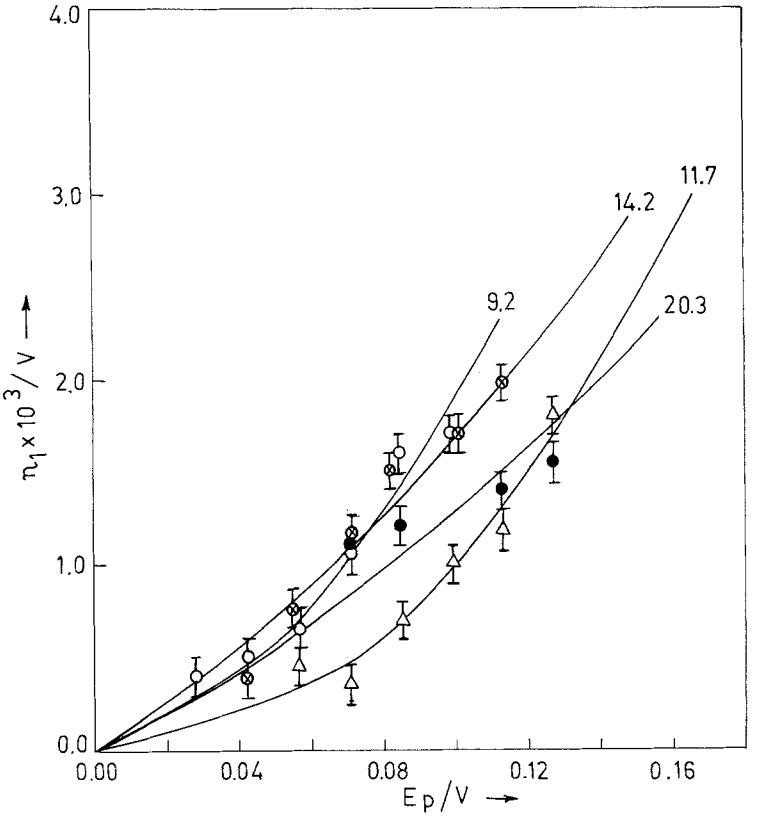

Fig. 6. Dependence of η_1 on E_p. System: same as in Fig. 3.

per the convention followed in the present work), at pH < 5 and anodic above that. This may be explained on the basis of the laws of electrode kinetics governing the corrosion reaction.

An expression for i_{cor} in terms of electrochemical parameters may be formulated as [11],

$$i = i_{0,c}\exp[-\alpha^r(E - E_c^r)] - i_{0,m} \times \exp[\beta^r(E - E_m^r)] \quad (13)$$

where $(i_{0,c}; i_{0,m})$ and $(E_c^r; E_m^r)$ represent the exchange current and the equilibrium potential for cathodic conjugate (subscript c) and anodic metal dissolution (subscript m) reactions, respectively; $\alpha^r = 2.303/b_c^r$ and $\beta^r = 2.303/b_m^r$, where b_c^r and b_m^r are the cathodic and anodic Tafel slopes, respectively.

When the alternating potential $[E_p\cos(\omega t - \phi)]$ is applied across the system, the mean potential of the electrode changes from E_{cor} to E_1, and

$$\tilde{i} + \bar{i} = i_{0,c}\exp[-\alpha^r\{(E_1 - E_c^r) + E_p\cos(\omega t - \phi)\}] - i_{0,m}\exp[\beta^r\{(E_1 - E_m^r) + E_p\cos(\omega t - \phi)\}] \quad (14)$$

where $\tilde{i}$ is the alternating current passing through the system. Separating the a.c. and d.c. terms in this, in the same way as shown earlier [1],

$$\bar{i} = i_{0,c}I_0(\alpha^r E_p)\exp[-\alpha^r(E_1 - E_c^r)] - i_{0,m}I_0(\beta^r E_p)\exp[\beta^r(E_1 - E_m^r)] \quad (15)$$

where $I_0(\alpha^r E_p)$ and $I_0(\beta^r E_p)$ are modified Bessel functions of the first kind and order zero.

It is evident from a first look at Equation 15 that $\bar{i} \gtrless 0$ according to $\alpha^r \gtrless \beta^r$. Sathyanarayana, in his original work on the faradaic rectification method for i_{cor} measurements, also arrived at a similar conclusion [4].

If the observed effect of pH on $\bar{i}$ (Fig. 15) were to be explained on this basis, one should assume that α^r progressively decreases with increase in pH. However, it may be seen from Fig. 2 that the cathodic Tafel lines have similar slopes both at pH 1 and 1.9 (Further experiments showed hardly

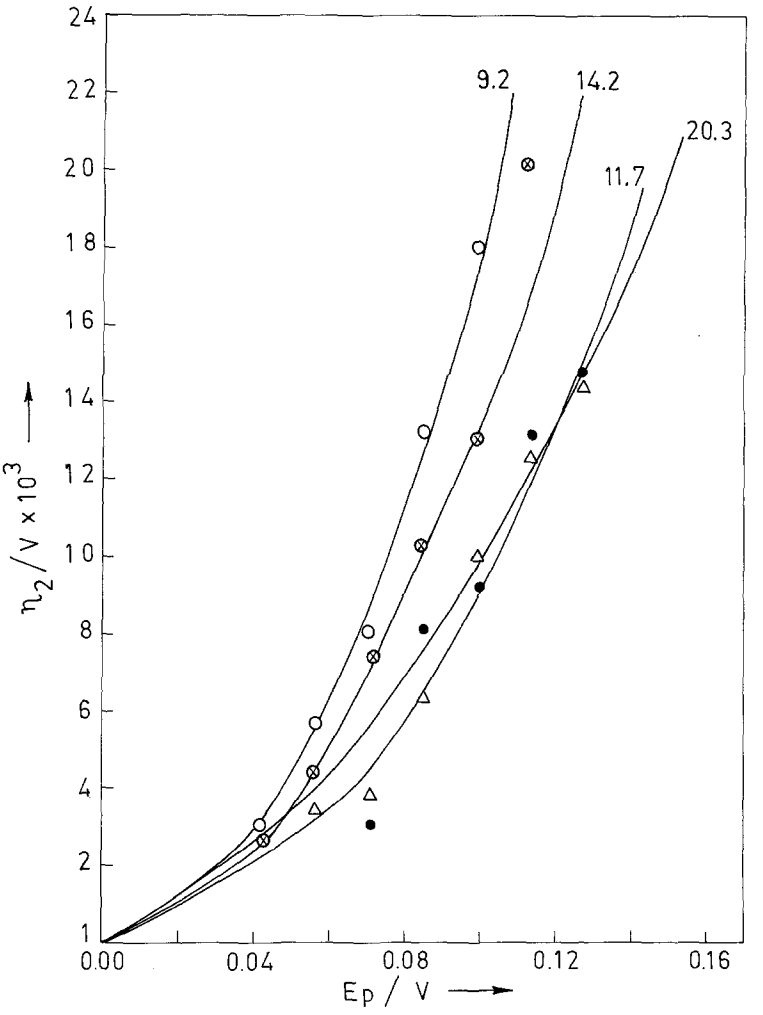

Fig. 7. Dependence of η_2 on E_p. System: same as in Fig. 3.

any variation in the cathodic Tafel slope with pH in the range of 0.9 to 6.0). Thus there is hardly any variation in α^r with pH. Hence $\bar{i}$ cannot depend upon α^r or β^r, at least in the present case.

Thus, it must be concluded from Equation 15 that the magnitude and direction of $\bar{i}$ should almost completely be determined according to the inequality relation between $i_{0,c}$ and $i_{0,m}$, i.e. $\bar{i} \gtrless 0$ according to $i_{0,c} \gtrless i_{0,m}$. This indeed is in agreement with the observations in the present case, if we further consider the well known relation [12].

$$i_{0,c} = Fk_s^c C_{O,c}^{(1-\alpha^r)} C_{R,c}^{\alpha^r} \qquad (16)$$

where k_s^c is the standard rate constant; $C_{O,c}$ is the concentration of the oxidant and $C_{R,c}$ that of the reductant. Now, if $C_{R,c}$ (i.e. the partial pressure of hydrogen) were to be kept a constant and only $C_{O,c}$ (the hydrogen ion concentration) were to be decreased, $i_{0,c}$ should progressively decrease. This decrease, in the present case, taken in conjunction with a constant $i_{0,m}$, reasonably well explains the variation of $\bar{i}$ with pH.

4.5. *Effect of dissolved oxygen on the direction of rectification*

A set of faradaic rectification measurements were also made with the above system (oxide film thickness, $x = 8$ nm and electrolyte pH = 1.9), just before the cathodic polarization treatment. $\bar{i}$ was found to be anodic and of much smaller magnitude as compared to the one observed after the cathodic treatment (Fig. 15). This effect is most

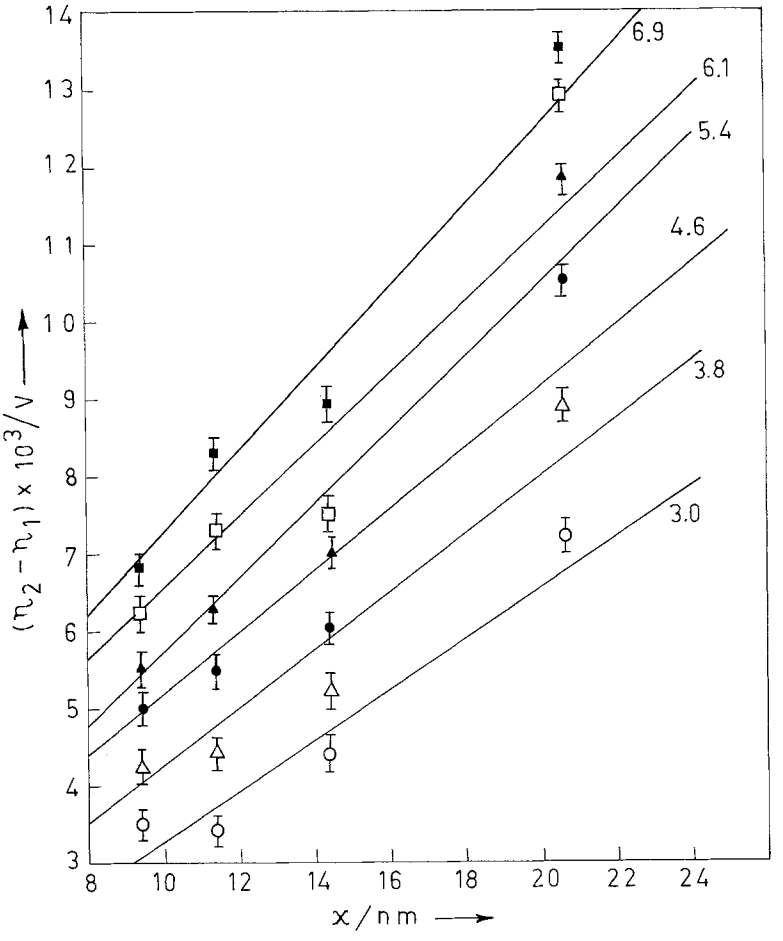

Fig. 8. Variation of $\eta_2 - \eta_1$ with x. System: Same as in Fig. 3. Numbers on the curves represent $\bar{i}$ in $\times 10^2$ A m^{-2}.

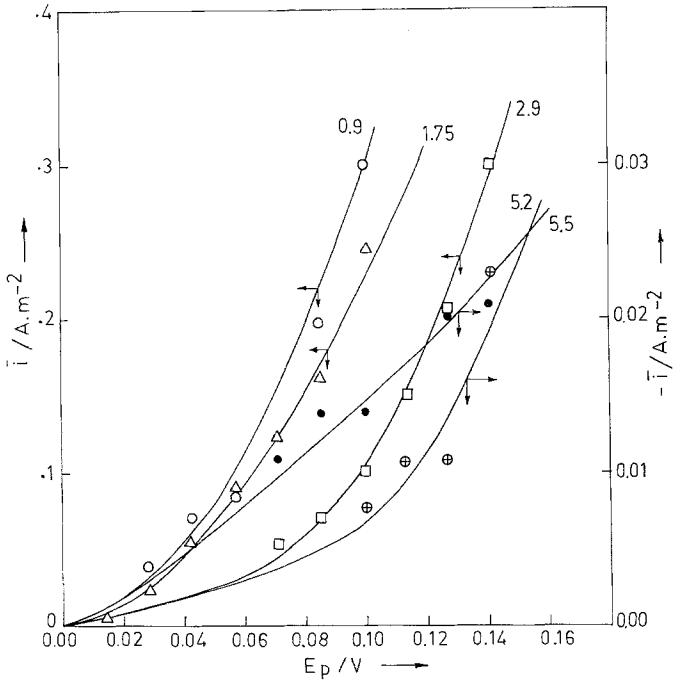

Fig. 9. Dependence of $\bar{i}$ on E_p. Numbers on the curve represent the pH of the electrolyte. System: zone refined aluminium/oxide/1 mol dm^{-3} sodium sulphate; oxide film thickness = 8 nm.

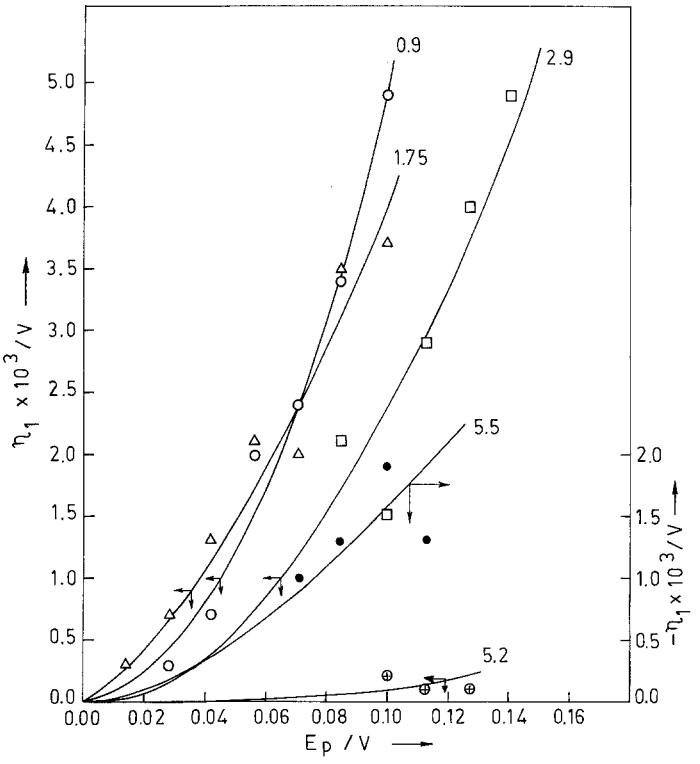

Fig. 10. Dependence of η_1 on E_p. Other details same as in Fig. 9.

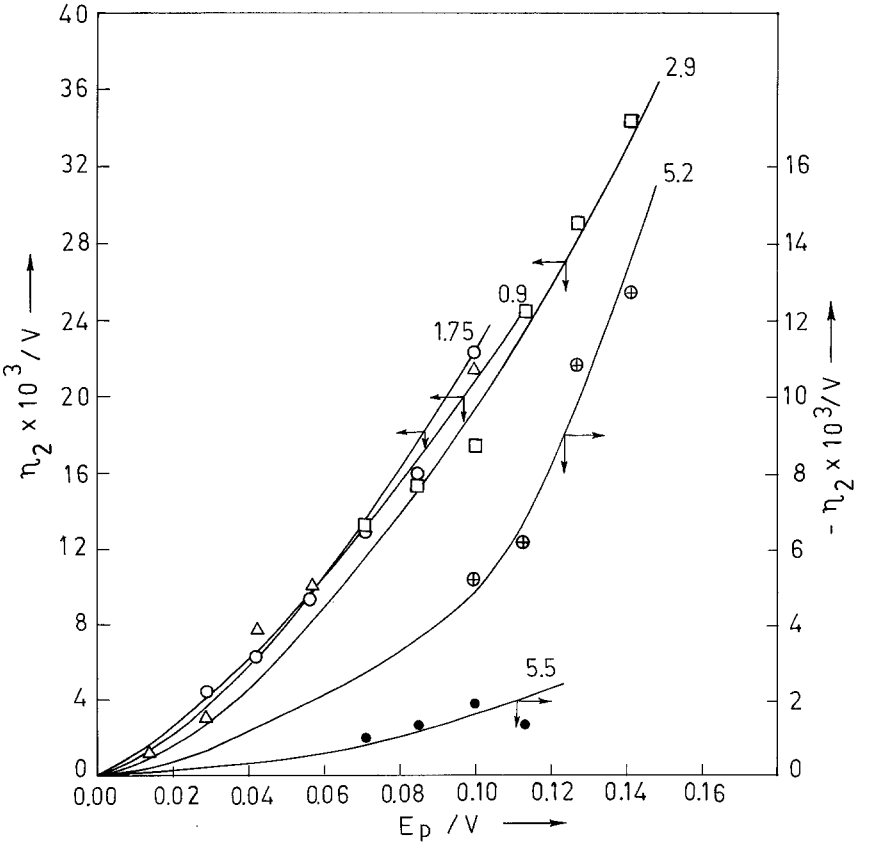

Fig. 11. Dependence of η_2 on E_p. Other details same as in Fig. 9.

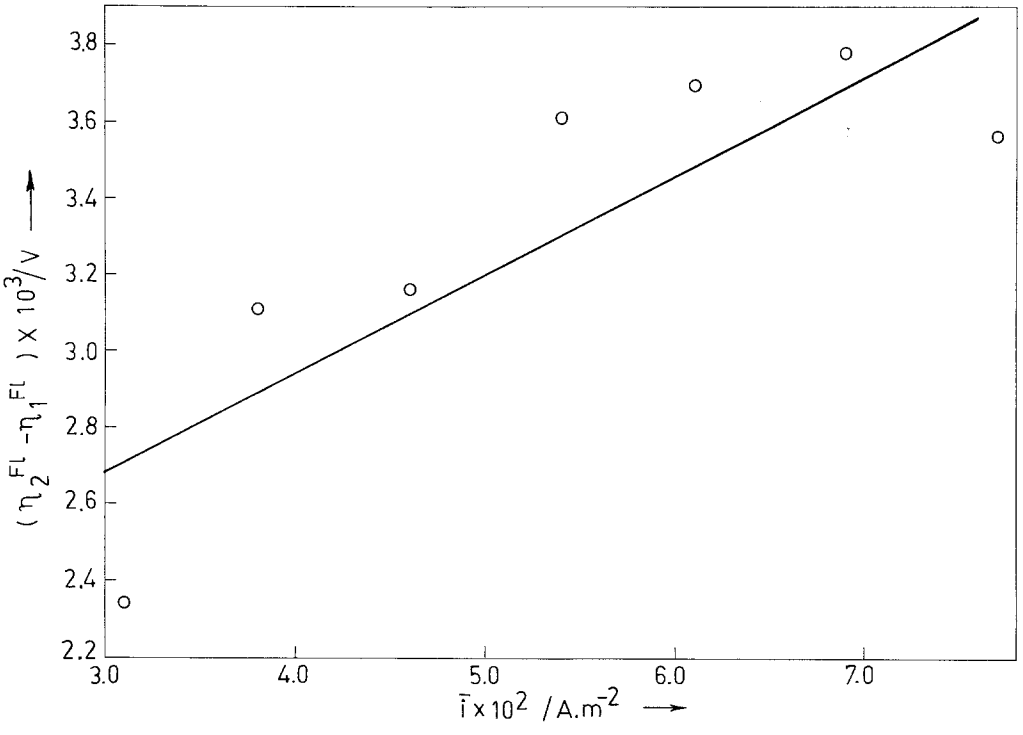

Fig. 12. Variation of $(\eta_2^{Fl} - \eta_1^{Fl})$ with $\bar{i}$.

likely due to the absorbed oxygen at the oxide/electrolyte interface (and not removed during deaeration), which might have been reduced during the cathodic polarization. It was therefore decided to investigate the effect of oxygen in the electrolyte on $\bar{i}$. As may be seen from Fig. 15, this resulted in a distinct increase in $\bar{i}$ in the anodic direction. (The $\bar{i}$ values measured with both the deaerated as well as oxygen saturated electrolyte were irreproducible, although it was more anodic in the latter case. It was for this reason that the electrode was given a cathodic treatment prior to the rectification and a.c. impedance measurements (cf. Section 3.1). $\bar{i}$ values were found reproducible after such a treatment. A cathodic current of 30 A m^{-2} over a duration of 150 min was found adequate for this purpose, at all values of x; any further increase in the current or time did not alter the value of $\bar{i}$).

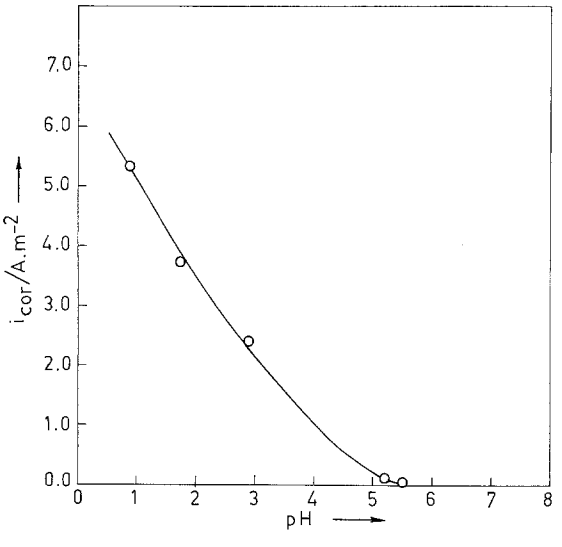

Fig. 13. Dependence of i_{cor} on pH. System: same as in Fig. 9.

If oxygen reduction were to be the main cathodic reaction (at pH = 1.9) such variations in $\bar{i}$ with the concentration of the dissolved oxygen can neither be explained on the basis of increasing α^x nor the increasing $i_{0,c}$ with increasing oxygen concentration.

It is hence likely that oxygen does not act as a depolarizer in the corrosion reaction of aluminium, but instead gets adsorbed at the oxide/electrolyte interface and inhibits the hydrogen evolution reaction. Thus, $i_{0,c}$, the equilibrium

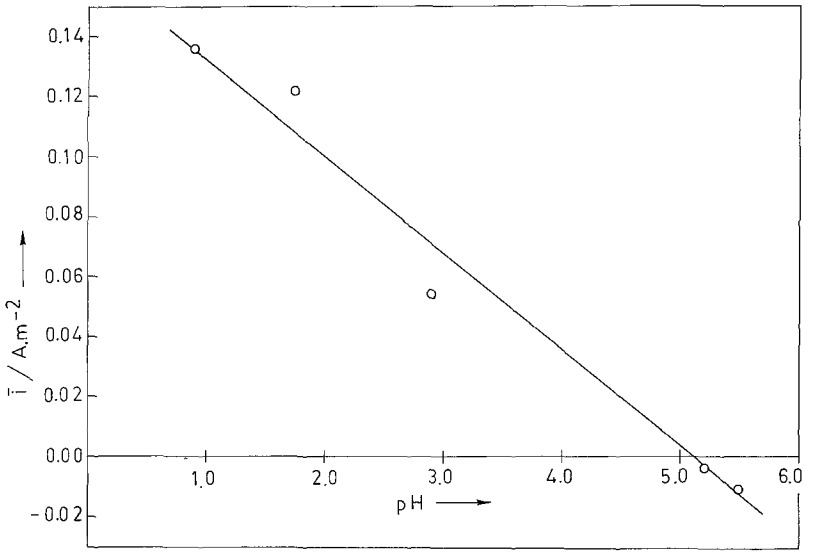

Fig. 14. Dependence of $\bar{i}$ on pH as measured at E_p = 70 mV. System: same as in Fig. 9.

exchange current for hydrogen evolution reaction (in Equation 15) is modified according to the activity of the adsorbed oxygen, resutling in the reversal of $\bar{i}$.

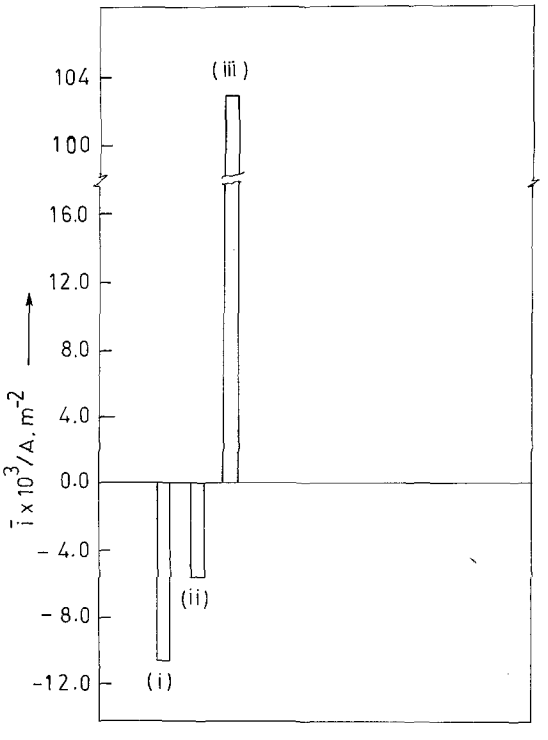

Fig. 15. Effect of dissolved oxygen on $\bar{i}$ at E_p = 70 mV. System: Zone refined aluminium/oxide/1 mol dm^{-3}. Sodium sulphate (pH = 1.9); oxide films thickness = 8 nm. (i) Electrolyte saturated with oxygen. (ii) Electrolyte deaerated. (iii) Electrolyte deaerated and electrode cathodically polarized with a current 30 A m^{-2} for 150 min before $\bar{i}$ measurements.

5. Conclusion

The surface oxide film on aluminium can substantially interfere with measurement of its corrosion rate because of the impedance and potential drop across the oxide. Then, correction for the potential drop across the oxide is possible, although not trivial. The present method based on faradaic rectification and a.c. impedance demonstrates such a possibility. The procedure for this purpose is rather elaborate as compared to the faradaic rectification method for a metal/electrolyte system [4]. However, the method also helps to characterize the oxide film in terms its impedance and rectification properties. Once this is done in one electrolyte, it should be possible to evaluate the corrosion rate of the electrode in any other electrolyte; only faradaic rectification measurements are necessary for this purpose.

Thus, in the above study, the evaluation of corrosion rate after the correction for the potential drop across the anodic oxide on aluminium electrode in 1 mol dm^{-3} sodium sulphate at pH 1.9 was found to be possible, although the entire procedure was rather involved and time consuming. But having once identified the film impedance, $|Z_{Fl}|$ and the rectification potentials due to it (Fig. 12), i_{cor} was evaluated at all other pH values from faradaic rectification measurements alone. In the latter case the method was as instantaneous as the one proposed for metal/electrolyte systems [4].

Acknowledgements

The authors would like to thank Professor Hira Lal for useful discussions and Messrs K. Sivaji and T. Murali for their help in programming and computation.

References

[1] R. Srinivasan and C. S. C. Bose, *J. Appl. Electrochem.* **13** (1983) 157.
[2] M. J. Dignam, 'Mechanism of Ionic Transport through Oxide Films' in 'Oxides and Oxide Films' Vol. 1, edited by J. W. Diggle, Marcel Dekker, New York (1972) p. 97.
[3] R. Srinivasan and C. S. C. Bose, *J. Appl. Electrochem.* **12** (1982) 487.
[4] S. Sathyanarayana, *J. Electroanal. Chem.* **62** (1975) 209.
[5] R. Srinivasan and S. Sathyanarayana, *Brit. Corros. J.* **12** (1977) 221.
[6] B. N. Kabanov, I. I. Astakhov and I. G. Kisleva, *Russian Chem. Rev.* **34** (1965) 775.
[7] A. K. Vijh, 'Anodic Oxide Films: Infleunce of Solid State Properties on Electrochemical Behaviour in 'Oxide and oxide films', Vol. 2, edited by J. W. Diggle, Marcel Dekker, New York (1973) p. 75.
[8] R. E. Mayer, *J. Electrochem. Soc.* **107** (1960) 847.
[9] S. M. Ahmed, 'Electrical Double Layer at Metal Oxide Solution Interface', in 'Oxides and Oxide Films' Vol. 1, edited by J. W. Diggle, Marcel Dekker, New York (1972) p. 377 and other references cited therein.
[10] P. Carlsson and B. Holmstrom, *J. Electrochem. Soc.* **129** (1982) 1851.
[11] For example, J. O'M. Bockris and A. N. K. Reddy, 'Modern Electrochemistry', Vol. 2, Plenum Press, New York (1970) p. 1287.
[12] Paul Delahay, 'Double Layer and Electrode Kinetics', Interscience Publishers, New York (1965) p. 153.